

Solution of Mathieu's equation by Runge-Kutta integration

T.Funada,* J.Wang,[†] D.D.Joseph,^{†‡} N.Tashiro,* Y.Sonoda*

*Department of Digital Engineering, Numazu College of Technology, 3600 Ooka, Numazu, Shizuoka, 410-8501, Japan [†]Department of Aerospace Engineering and Mechanics, University of Minnesota, 110 Union St. SE, Minneapolis, MN 55455, USA

In this note we shall show that Mathieu's equation for $x(t)$

$$\ddot{x} + [p - 2q \cos(2t)]x = 0$$

may be efficiently and accurately integrated by the Runge-Kutta (RK) method under the initial conditions

$$x = 1, \quad \dot{x} = 0$$

for the even Mathieu functions $ce_n(t, q) \rightarrow \cos(nt)$ as $q \rightarrow 0$ and

$$x = 0, \quad \dot{x} = 1$$

for the odd Mathieu functions $se_n(t, q) \rightarrow \sin(nt)$ as $q \rightarrow 0$.

1 Some properties of the Mathieu functions

The properties of Mathieu's functions which we shall generate by RK integration are very briefly described in the caption of figure 1.

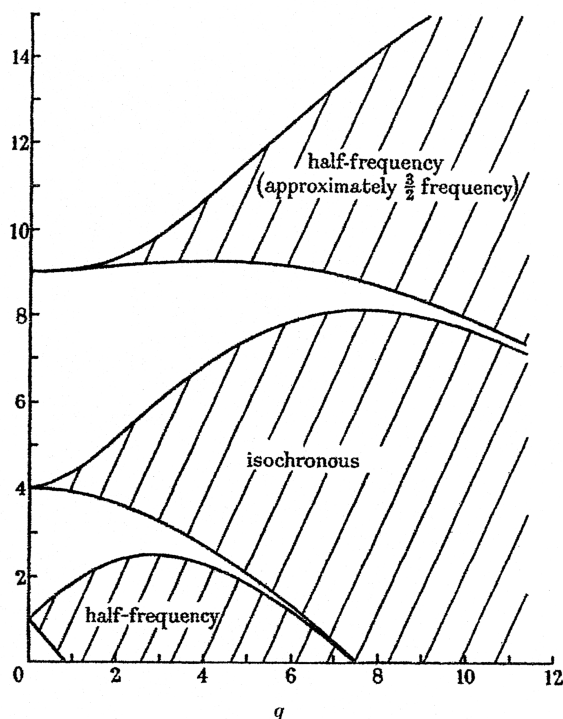


Figure 1. Stability chart for the solutions of Mathieu's equation. The shaded regions are unstable with $x(t) = e^{\gamma t} f(t)$, $\gamma > 0$, $f(t) = f(t + 2\pi)$ in the half frequency region, $f(t) = f(t + \pi)$ in the isochronous region and $f(t) = f(t + 2\pi)$ in the 3/2 frequency region. The marginal states are borders of stable-unstable regions on which $\gamma = 0$ and the characteristic value is given by $p = p(q)$. The solutions in stable regions are oscillatory though not regularly periodic.

[‡]Author to whom correspondence should be addressed. Telephone: (612) 625-0309; fax (612) 626-1558; electronic mail: joseph@aem.umn.edu

2 Numerical method

In the fourth order RK integration, we may take the time difference $\Delta t = \pi/2^{12} = \pi/4096$ for which time at n steps is given by $t = n \times \Delta t$ and a periodic time T may be defined as

$$T = \left[\frac{t}{2\pi} \right] \quad (2.1)$$

with Gauss' symbol $[]$. According to Floquet theory, we may represent the solutions of Mathieu's equation in the unstable region as

$$\log x(t) = \gamma t + b = \gamma 2\pi T + b \quad (2.2)$$

where $b = f(t)$ is periodic in t but constant in T , and the growth rate γ is positive. The growth rate $\gamma = 0$ at the marginal state. To check $b = f(t)$, we may use Fourier series expressed as

$$f(t) = \sum_{n=-\infty}^{\infty} A_n \exp(int) \quad (2.3)$$

where the Fourier coefficient A_{-n} is the complex conjugate of A_n . The coefficient is evaluated as

$$A_m = \frac{1}{2\pi} \int_t^{t+2\pi} f(t) \exp(-imt) dt = \frac{1}{2\pi} \sum_{j=1}^{8192} [f(t_j) \exp(-imt_j) + f(t_{j-1}) \exp(-imt_{j-1})] \frac{\Delta t}{2} \quad (2.4)$$

with the trapezoidal rule, $t_j = t + j \times \Delta t$.

In tables 1 and 2 we give the values of γ and b in the Floquet formula (2.2) for the eight cases marked on figure 2, where $p = 2q$ is a representative function. Graphs of $f(t)$ for the eight cases are shown in figures in the following sections.

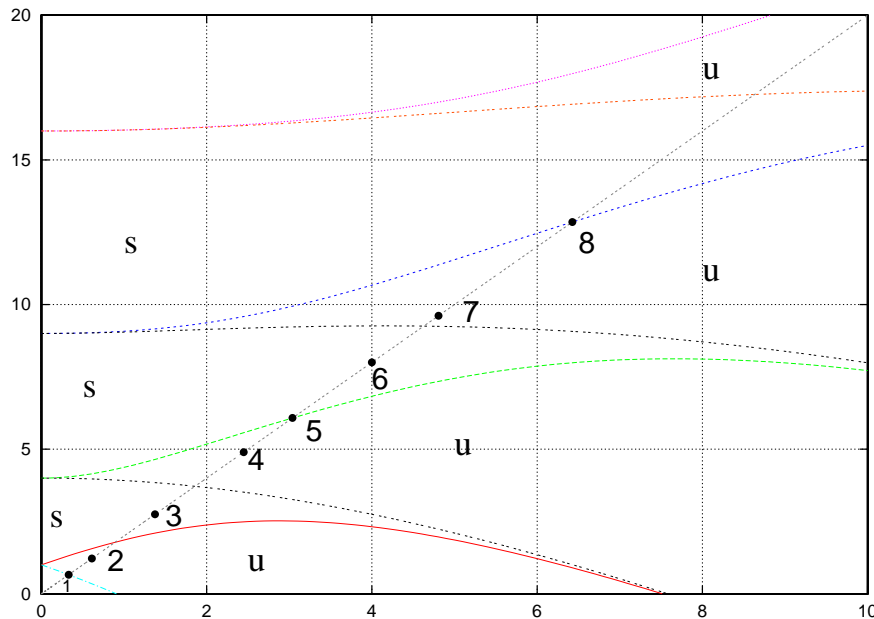


Figure 2. Points on stability diagrams computed by RK integration (see tables 1, 2 and figures in the following sections). “u” denotes unstable region and “s” denotes stable region. $p = 2q$. Points 1, 5, 8 are at the marginal state with periodic solutions, which can be expressed by the Mathieu functions $ce_n(t, q)$ or $se_n(t, q)$ on the borders; point 1 is on the Mathieu function $se_1(t, q)$, point 5 is on the Mathieu function $ce_2(t, q)$ and point 8 is on $ce_3(t, q)$. Points 2, 4, 7 are in unstable region with exponential growth. The solutions at points 3, 6 in stable region are oscillatory though not regularly periodic.

After an initial transient, the numerical solutions approach asymptotic states which are independent of initial conditions. The data in table 1 are in the interval $10\pi \leq t \leq 100\pi$. The data in unstable regions and on the borders are reproduced well in table; this table shows a very high computation accuracy. The data in the stable region in table 1 is not the same as in table 2; this means the oscillatory solutions are not regularly periodic, the growth rate takes some small positive values and a negative value, but the amplitude of oscillation does not grow in time.

Table 1. γ, b for point 1–8 in $10\pi \leq t \leq 100\pi$.

| point | q | p | γ | b | t |
|---------------|-----------|-----------|------------|-----------|----------------------------|
| 1 (figure 3) | 3.290E-01 | 6.580E-01 | -4.265E-10 | 2.844E-08 | $10\pi \leq t \leq 100\pi$ |
| 2 (figure 8) | 6.094E-01 | 1.219E+00 | 0.2520 | -0.6931 | $10\pi \leq t \leq 100\pi$ |
| 3 (figure 6) | 1.374E+00 | 2.748E+00 | 4.150E-04 | -0.7527 | $10\pi \leq t \leq 100\pi$ |
| 4 (figure 9) | 2.449E+00 | 4.897E+00 | 0.2663 | -0.6931 | $10\pi \leq t \leq 100\pi$ |
| 5 (figure 4) | 3.039E+00 | 6.078E+00 | -2.891E-10 | 1.928E-08 | $10\pi \leq t \leq 100\pi$ |
| 6 (figure 7) | 4.000E+00 | 8.000E+00 | 2.894E-04 | -0.7612 | $10\pi \leq t \leq 100\pi$ |
| 7 (figure 10) | 4.807E+00 | 9.614E+00 | 0.1687 | -0.6931 | $10\pi \leq t \leq 100\pi$ |
| 8 (figure 5) | 6.426E+00 | 1.285E+01 | -1.164E-10 | 7.759E-09 | $10\pi \leq t \leq 100\pi$ |

Table 2. γ, b for point 1–8 in $100\pi \leq t \leq 1000\pi$. The argument in exponential function used in the computations should be less than 709.782 in double precision.

| point | q | p | γ | b | t |
|--------------|-----------|-----------|------------|-----------|------------------------------|
| 1 | 3.290E-01 | 6.580E-01 | -4.265E-09 | 2.861E-06 | $100\pi \leq t \leq 1000\pi$ |
| 2 | 6.094E-01 | 1.219E+00 | 0.2520 | -0.6931 | $100\pi \leq t \leq 800\pi$ |
| 3 (figure 6) | 1.374E+00 | 2.748E+00 | 1.710E-06 | -0.6987 | $100\pi \leq t \leq 1000\pi$ |
| 4 | 2.449E+00 | 4.897E+00 | 0.2663 | -0.6892 | $100\pi \leq t \leq 800\pi$ |
| 5 | 3.039E+00 | 6.078E+00 | -2.891E-09 | 1.939E-06 | $100\pi \leq t \leq 1000\pi$ |
| 6 (figure 7) | 4.000E+00 | 8.000E+00 | -5.887E-06 | -0.6821 | $100\pi \leq t \leq 1000\pi$ |
| 7 | 4.807E+00 | 9.614E+00 | 0.1687 | -0.6931 | $100\pi \leq t \leq 1000\pi$ |
| 8 | 6.426E+00 | 1.285E+01 | -1.164E-09 | 7.805E-07 | $100\pi \leq t \leq 1000\pi$ |

3 Periodic solutions

The oscillation patterns for the periodic solutions for points 1, 5 and 8 in figure 2 are shown in figures 3, 4, 5. Values of the largest Fourier components $> 10^{-4}$ are presented in tables 3, 4 and 5. The number of active Fourier modes increases with q . The aim of these tables is to show the accuracy of our computations.

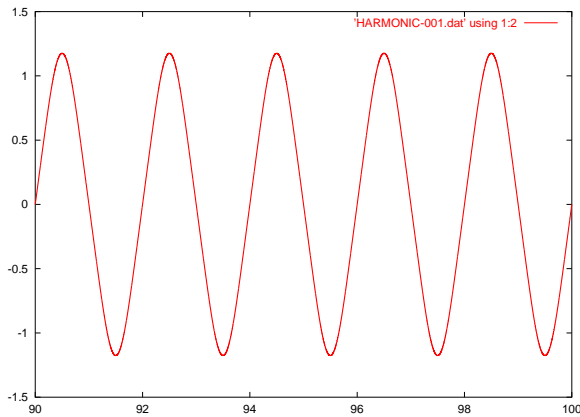


Figure 3. $f(t)$ versus t/π for $q = 3.290\text{E}-01$, $p = 6.580\text{E}-01$ (point 1, periodic $se_1(t, q)$), $90\pi \leq t \leq 100\pi$.

Table 3. Spectrum for the stable point 1 in the interval $30\pi < t \leq 100\pi$.

| k | $\text{Re}(A_k)$ | $\text{Im}(A_k)$ |
|-----|------------------|------------------|
| 1 | — | -5.654e-01 |
| 3 | — | 2.231e-02 |
| 5 | — | -3.016e-04 |

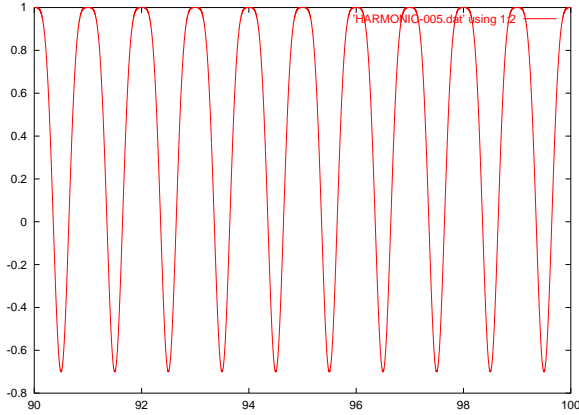


Figure 4. $f(t)$ versus t/π for $q = 3.039$, $p = 6.078$ (point 5, periodic $ce_2(t, q)$), $90\pi \leq t \leq 100\pi$.

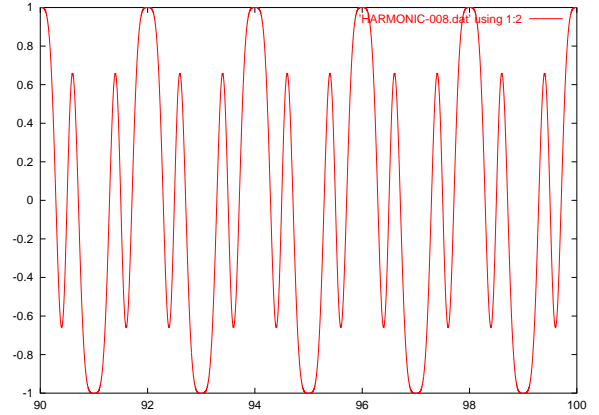


Figure 5. $f(t)$ versus t/π for $q = 6.426$, $p = 1.285E+01$ (point 8, periodic $ce_3(t, q)$), $90\pi \leq t \leq 100\pi$.

Table 4. Spectrum for point 5 in $30\pi < t \leq 100\pi$.

| k | $\text{Re}(A_k)$ | $\text{Im}(A_k)$ |
|-----|------------------|------------------|
| 0 | 4.117e-01 | — |
| 2 | 4.117e-01 | — |
| 4 | -1.302e-01 | — |
| 6 | 1.329e-02 | — |
| 8 | -6.986e-04 | — |

Table 5. Spectrum for point 8 in $30\pi < t \leq 100\pi$.

| k | $\text{Re}(A_k)$ | $\text{Im}(A_k)$ |
|-----|------------------|------------------|
| 1 | 3.492e-01 | — |
| 3 | 2.949e-01 | — |
| 5 | -1.725e-01 | — |
| 7 | 3.118e-02 | — |
| 9 | -2.957e-03 | — |
| 11 | 1.761e-04 | — |

4 Stable solutions

The stable solutions at point 3, 6 are displayed in figures 6, 7 and decomposed into the spectra A_0 - A_{20} in tables 6, 7; A_n for $n > 20$ has been cut off, though it still takes values of order 10^{-4} . These provide the evidence that the solutions are not periodic.

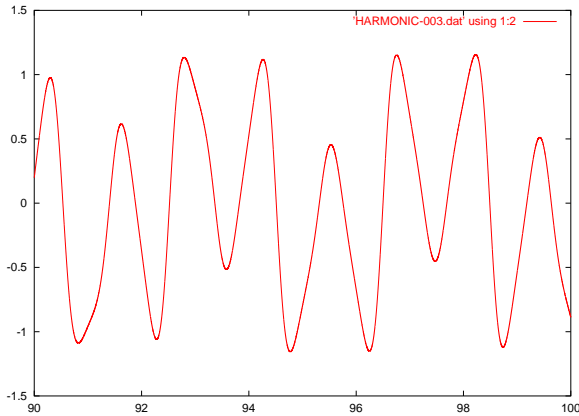


Figure 6a. $f(t)$ versus t/π for $q = 1.374$, $p = 2.748$ (point 3, stable), $90\pi \leq t \leq 100\pi$.

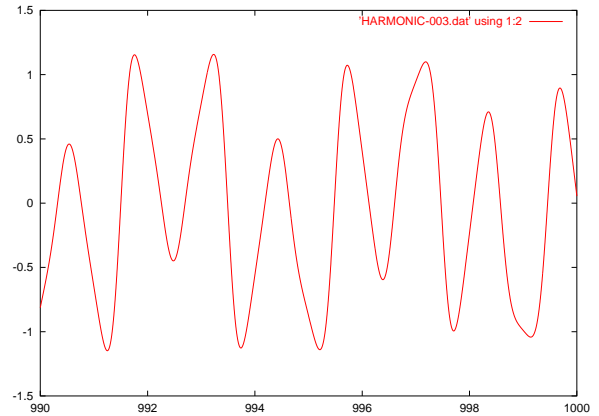


Figure 6b. $f(t)$ versus t/π for $q = 1.374$, $p = 2.748$ (point 3, stable), $990\pi \leq t \leq 1000\pi$.

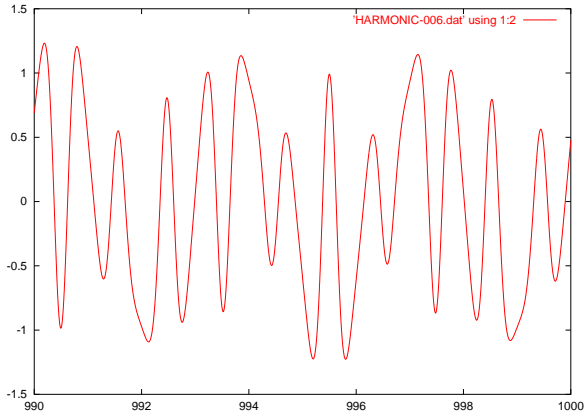
Table 6. Spectrum for point 3 in $990\pi \leq t \leq 1000\pi$.

| k | $\text{Re}(A_k)$ | $\text{Im}(A_k)$ |
|-----|------------------|------------------|
| 0 | -1.076e-02 | — |
| 1 | 6.497e-02 | -3.205e-03 |
| 2 | -3.099e-02 | 4.007e-02 |
| 3 | -2.251e-02 | 1.282e-02 |
| 4 | -4.251e-04 | 3.696e-03 |
| 5 | -6.614e-04 | 5.171e-03 |
| 6 | -1.250e-03 | 4.688e-03 |
| 7 | -7.977e-04 | 3.934e-03 |
| 8 | -5.054e-04 | 3.438e-03 |
| 9 | -3.285e-04 | 3.061e-03 |
| 10 | -2.005e-04 | 2.756e-03 |
| 11 | -1.043e-04 | 2.506e-03 |
| 12 | — | 2.297e-03 |
| 13 | — | 2.119e-03 |
| 14 | — | 1.966e-03 |
| 15 | 1.062e-04 | 1.837e-03 |
| 16 | 1.369e-04 | 1.719e-03 |
| 17 | 1.613e-04 | 1.621e-03 |
| 18 | 1.803e-04 | 1.529e-03 |
| 19 | 2.017e-04 | 1.447e-03 |
| 20 | 2.138e-04 | 1.375e-03 |

Figure 7. $f(t)$ versus t/π for $q = 4.000$, $p = 8.000$ (point 6, stable), $990\pi \leq t \leq 1000\pi$.

Table 7. Spectrum for point 6 in $990\pi \leq t \leq 1000\pi$.

| k | $\text{Re}(A_k)$ | $\text{Im}(A_k)$ |
|-----|------------------|------------------|
| 0 | -4.847e-03 | — |
| 1 | 1.618e-03 | -3.183e-03 |
| 2 | -3.832e-03 | 2.937e-04 |
| 3 | 3.258e-03 | -1.043e-02 |
| 4 | 3.105e-03 | -3.069e-03 |
| 5 | -2.659e-04 | 7.484e-04 |
| 6 | -1.056e-04 | -8.807e-04 |
| 7 | 2.808e-04 | -1.149e-03 |
| 8 | 2.115e-04 | -8.487e-04 |
| 9 | 1.564e-04 | -7.322e-04 |
| 10 | 1.394e-04 | -6.691e-04 |
| 11 | 1.276e-04 | -6.092e-04 |
| 12 | 1.154e-04 | -5.584e-04 |
| 13 | 1.098e-04 | -5.147e-04 |
| 14 | 1.029e-04 | -4.785e-04 |
| 15 | — | -4.466e-04 |
| 16 | — | -4.185e-04 |
| 17 | — | -3.926e-04 |
| 18 | — | -3.744e-04 |
| 19 | — | -3.523e-04 |
| 20 | — | -3.355e-04 |



5 Unstable solutions

Unstable solutions are periodic with increasing amplitude; the oscillation patterns are exhibited in figures 8, 9, 10 and in tables 8, 9, 10.

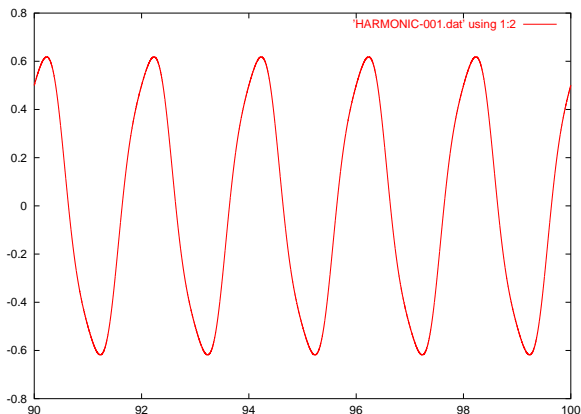


Figure 8. $f(t)$ versus t/π for $q = 6.094E-01$, $p = 1.219$ (point 2, unstable), $90\pi \leq t \leq 100\pi$.

Table 8. Spectrum for point 2 in $30\pi < t \leq 100\pi$.

| k | $\text{Re}(A_k)$ | $\text{Im}(A_k)$ |
|-----|------------------|------------------|
| 1 | 2.724e-01 | -1.490e-01 |
| 3 | -2.298e-02 | 7.271e-03 |
| 5 | 6.046e-04 | -1.227e-04 |

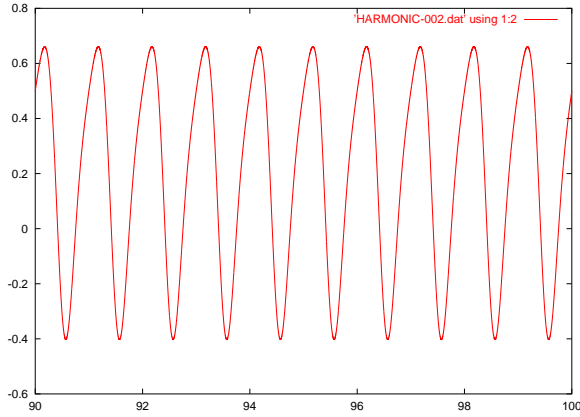


Figure 9. $f(t)$ versus t/π for $q = 2.449$, $p = 4.897$ (point 4, unstable), $90\pi \leq t \leq 100\pi$.

Table 9. Spectrum for point 4 in $30\pi < t \leq 100\pi$.

| k | $\text{Re}(A_k)$ | $\text{Im}(A_k)$ |
|-----|------------------|------------------|
| 0 | 1.952e-01 | — |
| 2 | 1.980e-01 | -1.545e-01 |
| 4 | -4.970e-02 | 2.504e-02 |
| 6 | 4.097e-03 | -1.559e-03 |
| 8 | -1.730e-04 | — |

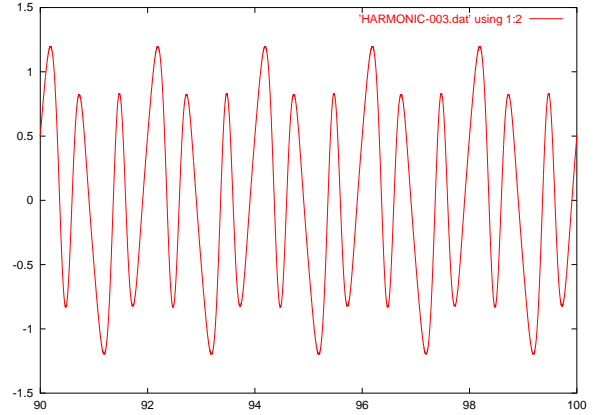


Figure 10. $f(t)$ versus t/π for $q = 4.807$, $p = 9.614$ (point 7, unstable), $90\pi \leq t \leq 100\pi$.

Table 10. Spectrum for point 7 in $30\pi < t \leq 100\pi$.

| k | $\text{Re}(A_k)$ | $\text{Im}(A_k)$ |
|-----|------------------|------------------|
| 1 | 1.623e-01 | -1.464e-01 |
| 3 | 1.398e-01 | -3.982e-01 |
| 5 | -5.981e-02 | 1.226e-01 |
| 7 | 8.255e-03 | -1.460e-02 |
| 9 | -5.978e-04 | 9.608e-04 |

6 Dissipation

In many applications, the oscillations associated with Mathieu's equation are damped with a dissipative term $\epsilon\dot{x}$. The equation for $x(t)$

$$\ddot{x} + \epsilon\dot{x} + [p - 2q \cos(2t)]x = 0 \quad \text{with } x(0) = 1, \quad \dot{x}(0) = 0, \quad (6.1)$$

may be transformed, using

$$x = y \exp\left(-\frac{\epsilon}{2}t\right), \quad (6.2)$$

to a Mathieu equation for $y(t)$

$$\ddot{y} + [p' - 2q \cos(2t)]y = 0 \quad \text{with } y(0) = 1, \quad \dot{y}(0) = \frac{\epsilon}{2}, \quad (6.3)$$

where

$$p' = p - \frac{\epsilon^2}{4}. \quad (6.4)$$

Another problem (**Problem 2**) may be given by replacing the initial conditions by

$$x(0) = 0, \quad \dot{x}(0) = 1 \quad \rightarrow \quad y(0) = 0, \quad \dot{y}(0) = 1. \quad (6.5)$$

For both positive and negative values of ϵ , p is shifted to p' and the initial condition is the same in the latter **Problem 2**. The type of solutions $y(t)$ is determined by q and p' . In the former **Problem 1**, the initial condition also includes ϵ . The problem is different for positive or negative value of ϵ .

If a point (q, p) is given by the characteristic value $p = p(q)$ corresponding to $ce_n(t, q)$ (**Problem 1** when $\epsilon = 0$), the shifted point (q, p') is in unstable region. Thus we have the solution $y(t)$ such as

$$\ln |y| = \gamma' t + b', \quad (6.6)$$

where for $\gamma' > 0$, $f(t) = y(t)e^{-\gamma' t}$ is periodic. Then $x(t) = y(t) \exp(-\frac{\epsilon}{2}t) = f(t) \exp[(\gamma' - \frac{\epsilon}{2})t]$.

If a point (q, p) is given by the characteristic value $p = p(q)$ corresponding to $se_n(t, q)$ (**Problem 2** when $\epsilon = 0$), the shifted point $(q, p - \epsilon^2/4)$ is in stable region. Thus we have the solution $y(t)$ such as

$$\ln |y| = \alpha' t + b', \quad (6.7)$$

by which $y(t)$ looks like “beat” due to the tuning α' ; a long period may arise against the fundamental period π or 2π .

In table 11, we compare damped solutions with different damping constants $\epsilon = 0.01, 0.1, 0.3, 0.7$ for points 1, 5. In figures 11, 12, the difference between Problems 1 and 2 and between positive and negative values of ϵ can be found.

Table 11. Growth rate γ' for Problem 1 evaluated in the interval $100\pi \leq t \leq 1000\pi$. For $\epsilon = 0.01$, the interval is taken as $800\pi \leq t \leq 1000\pi$ to remove the initial transient.

| point | ϵ | q | p' | γ' |
|-----------------|------------|-----------|-----------|-----------|
| se ₁ | 0.1 | 3.290e-01 | 6.555e-01 | — |
| se ₂ | 0.1 | 1.858e+00 | 3.714e+00 | — |
| se ₃ | 0.1 | 4.627e+00 | 9.251e+00 | — |
| ce ₁ | 0.1 | 8.898e-01 | 1.777e+00 | 2.732e-02 |
| ce ₂ | 0.1 | 3.039e+00 | 6.076e+00 | 2.166e-02 |
| ce ₃ | 0.1 | 6.426e+00 | 1.285e+01 | 1.863e-02 |
| se ₁ | 0.3 | 3.290e-01 | 6.355e-01 | — |
| se ₂ | 0.3 | 1.858e+00 | 3.694e+00 | — |
| se ₃ | 0.3 | 4.627e+00 | 9.231e+00 | — |
| ce ₁ | 0.3 | 8.898e-01 | 1.757e+00 | 8.173e-02 |
| ce ₂ | 0.3 | 3.039e+00 | 6.056e+00 | 6.483e-02 |
| ce ₃ | 0.3 | 6.426e+00 | 1.283e+01 | 5.578e-02 |
| se ₁ | 0.7 | 3.290e-01 | 5.355e-01 | — |
| se ₂ | 0.7 | 1.858e+00 | 3.594e+00 | — |
| se ₃ | 0.7 | 4.627e+00 | 9.131e+00 | — |
| ce ₁ | 0.7 | 8.898e-01 | 1.657e+00 | 1.879e-01 |
| ce ₂ | 0.7 | 3.039e+00 | 5.956e+00 | 1.496e-01 |
| ce ₃ | 0.7 | 6.426e+00 | 1.273e+01 | 1.290e-01 |
| se ₁ | 0.01 | 3.290e-01 | 6.580e-01 | — |
| se ₂ | 0.01 | 1.858e+00 | 3.716e+00 | — |
| se ₃ | 0.01 | 4.627e+00 | 9.254e+00 | — |
| ce ₁ | 0.01 | 8.898e-01 | 1.780e+00 | 2.734e-03 |
| ce ₂ | 0.01 | 3.039e+00 | 6.078e+00 | 2.165e-03 |
| ce ₃ | 0.01 | 6.426e+00 | 1.285e+01 | 1.865e-03 |

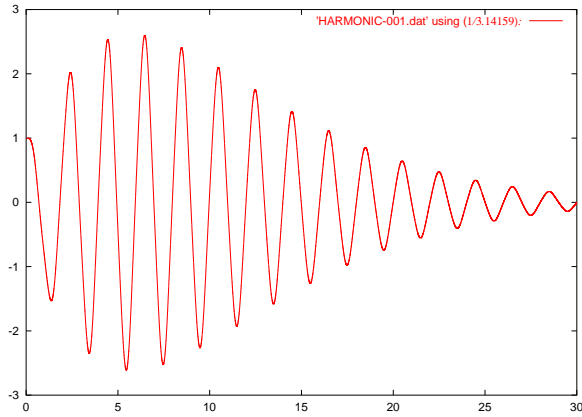


Figure 11a. $x(t)$ versus t/π for $(q, p') = (0.3290, 0.6555)$ shifted from point 1 and $\epsilon = 0.1$ in damped case, in $0 \leq t \leq 30\pi$.

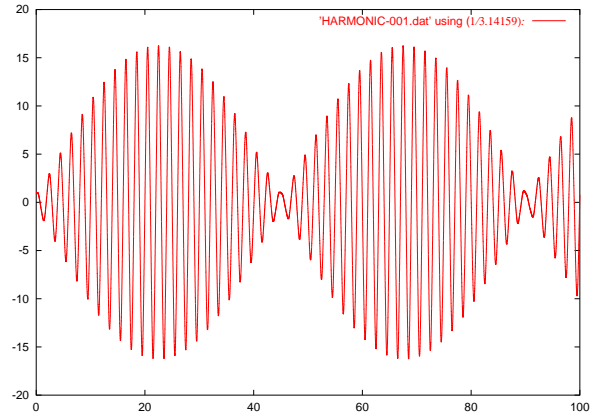


Figure 11b. $y(t)$ versus t/π for $(q, p') = (0.3290, 0.6555)$ shifted from point 1 and $\epsilon = 0.1$, in $0 \leq t \leq 100\pi$.

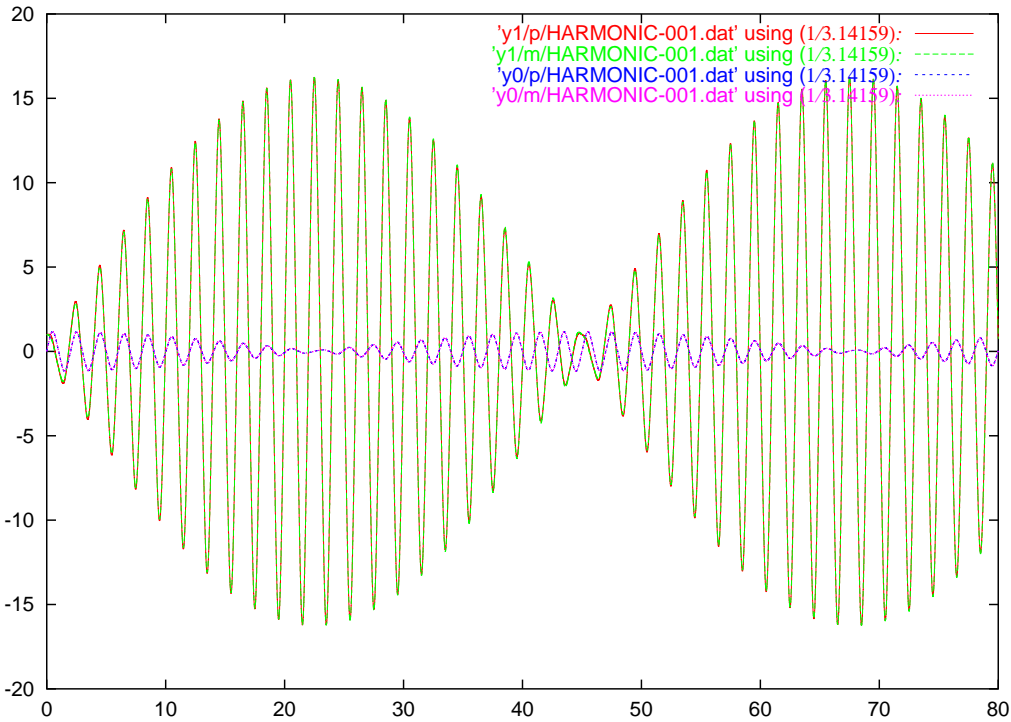


Figure 11c. $y(t)$ versus t/π for $(q, p') = (0.3290, 0.6555)$ shifted from point 1, in $0 \leq t \leq 80\pi$. Problem 1 with $\epsilon = 0.1$ (red), Problem 1 with $\epsilon = -0.1$ (green), Problem 2 with $\epsilon = 0.1$ (blue), Problem 2 with $\epsilon = -0.1$ (magenta). Problem 2 is the same for $\epsilon = \pm 0.1$.

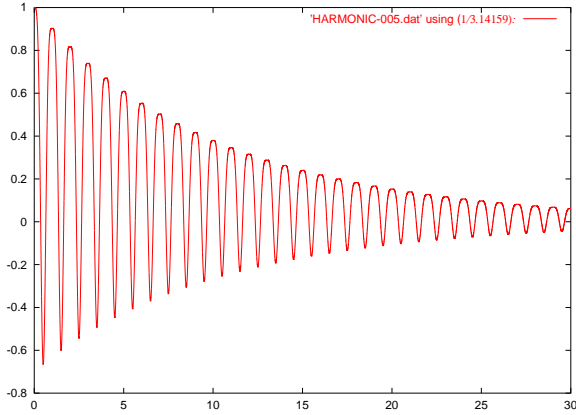


Figure 12a. $x(t)$ versus t/π for $(q, p') = (3.039, 6.076)$ shifted from point 5 and $\epsilon = 0.1$ in damped case, in $0 \leq t \leq 30\pi$.

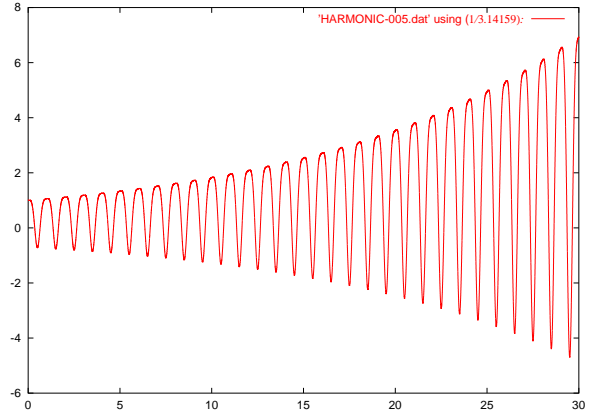


Figure 12b. $y(t)$ versus t/π for $(q, p') = (3.039, 6.076)$ shifted from point 5 and $\epsilon = 0.1$, in $0 \leq t \leq 30\pi$.

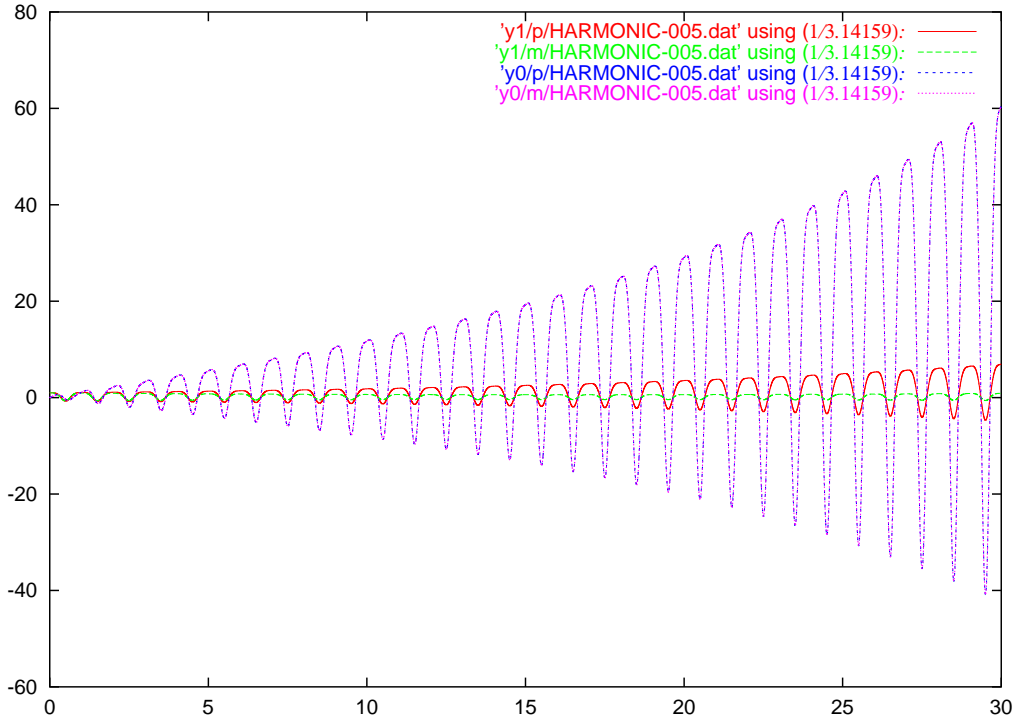


Figure 12c. $y(t)$ versus t/π for $(q, p') = (3.039, 6.076)$ shifted from point 5, in $0 \leq t \leq 30\pi$. Problem 1 with $\epsilon = 0.1$ (red), Problem 1 with $\epsilon = -0.1$ (green), Problem 2 with $\epsilon = 0.1$ (blue), Problem 2 with $\epsilon = -0.1$ (magenta). Problem 2 is the same for $\epsilon = \pm 0.1$.

The Runge-Kutta technique developed in this paper is a very fast and accurate method for solving problems governed by Mathieu's equation. Our work here was motivated by the need to develop an efficient method for developing a comprehensive study of irrotational Faraday waves on a viscous fluid.

This work was supported in part by the NSF under grants from Chemical Transport Systems.

References

- [1] Abramowitz, M. & Stegun, I.A. (ed.) 1972. *Handbook of Mathematical Functions with Formulas, Graphs, and Mathematical Tables*, U.S. Department of Commerce.

Contents

| | | |
|----------|---|----------|
| 1 | Some properties of the Mathieu functions | 1 |
| 2 | Numerical method | 2 |
| 3 | Periodic solutions | 3 |
| 4 | Stable solutions | 4 |
| 5 | Unstable solutions | 5 |
| 6 | Dissipation | 6 |